

ON THE DISCOVERY OF THE FIRST 350 MICRON-SELECTED GALAXY

SOPHIA A. KHAN^{1,2}, RICHARD A. SHAFER², DOMINIC J. BENFORD², JOHANNES G. STAGUHN^{2,3}, PIERRE CHANIAL^{2,4},
EMERIC LE FLOC'H⁵, THOMAS S. R. BABBEDGE¹, DUNCAN FARRAH^{6,7}, S. HARVEY MOSELEY², ELI DWEK², DAVID L. CLEMENTS¹,
TIMOTHY J. SUMNER¹, MATTHEW L. N. ASHBY⁸, KATE BRAND⁹, MARK BRODWIN¹⁰, PETER R. EISENHARDT¹⁰,
RICHARD ELSTON^{11,12}, ANTHONY H. GONZALEZ¹¹, ERIC MCKENZIE¹¹, STEPHEN S. MURRAY⁸

Draft version November 26, 2018

ABSTRACT

We report the detection of a 3.6σ 350 μm -selected source in the Boötes Deep Field. The source, the first Short-wavelength Submillimeter-selected Galaxy (SSG 1), was discovered as part of a blank field extragalactic survey using the 350 μm -optimised Submillimeter High Angular Resolution Camera (SHARC II) at the Caltech Submillimeter Observatory. With multiwavelength photometry from NOAO-NDWFS (R and I band), FLAMEX (J and K_s), *Spitzer* (IRAC and MIPS) and the Westerbork 1.4 GHz Deep Survey (radio upper limit), we are able to constrain the photometric redshift using different methods, all of which suggest a redshift ~ 1 . In the absence of long-wavelength submillimeter data we use SED templates to infer that this source is an ultraluminous infrared galaxy (ULIRG) with a dust temperature of 30 ± 5 K, occupying a region of luminosity-temperature space shared by moderate redshift *ISO*-selected ULIRGs (rather than high redshift SCUBA-selected SMGs). SHARC II can thus select SMGs with moderately “warm” dust that might be missed in submillimeter surveys at longer wavelengths.

Subject headings: infrared: galaxies – submillimeter: galaxies – galaxies: starburst – galaxies: high-redshift

1. INTRODUCTION

Submillimeter-selected galaxies (SMGs) generally refer to the population detected in the pioneering lensed and blank deep field surveys using the Submillimeter Common User Bolometer Array (SCUBA; Holland et al. 1999) instrument on the James Clerk Maxwell Telescope (JCMT) (e.g., Smail, Ivison & Blain 1997; Hughes et al. 1998; Barger et al. 1998; Eales et al. 1999). They are regarded as the high redshift ($z \sim 2-3$; Chapman et al. 2005; Chapman et al. 2003; see also Simpson et al. 2004) counterparts to the population of luminous and ultraluminous infrared galaxies (LIRGs and ULIRGs) detected by the InfraRed Astronomical Satellite, *IRAS*, typically out to $z \lesssim 0.1$ (Soifer et al. 1984; Joseph & Wright 1985; and Soifer, Neugebauer & Houck 1987), since they share similar properties (fundamentally, that the bulk of the bolometric luminosity is emitted in the restframe far-IR, powered by a combination of star formation and AGN activity).

As a necessary consequence of the selection at longer submillimeter wavelengths, SMGs tend to have higher bolometric luminosities, and those with comparable luminosities to

IRAS-selected ULIRGs tend to have cooler dust temperatures (Blain et al. 2004). Between the two are the Infrared Space Observatory (*ISO*)-selected ULIRGs (Aussel et al. 1999; Rowan-Robinson et al. 1999; Elbaz et al. 2002a), which occupy an intermediate redshift space ($z \sim 1$), and have dust masses in-between the *IRAS* and SCUBA-selected ULIRGs (Chapman et al. 2002; Blain et al. 2004; this is also a region of parameter space that will be shared by *Spitzer*-selected galaxies, see, e.g., Yan et al. 2004).

Sources selected at 350 μm are expected to be predominantly LIRGs and ULIRGs at $1 < z < 3$ (the K-correction changes from negative to positive with increasing redshift as the observing window moves towards and past the Wien peak; see, e.g., Guiderdoni et al. 1998; Khan, 2005, in preparation). Galaxies at $z \sim 1$ are likely to be the dominant source of the integrated far-IR background (Puget et al. 1996; Fixsen et al. 1998; Elbaz et al. 2002b); also, observations suggest that after a relatively steep rise from $z=0$ to ~ 1 , the cosmic star formation rate (CSFR) appears to flatten off between $z=1$ and ~ 4 , with evidence for a slow decline at higher redshift (Lilly et al. 1996; Madau et al. 1996; Connolly et al. 1997; Steidel et al. 1999; Gabasch et al. 2004). Hence 350 μm -selected sources are an important probe of the epoch of peak star formation rate in the universe.

In this Letter we report on the detection of a single source above 3σ at 350 μm . It is, to the best of our knowledge, the first short-wavelength submillimeter-selected galaxy (200–500 μm) and is denoted as SSG 1 in this Letter (but by standard convention, SMM J143206.65+341613.4). SSG 1 is the first object discovered *purely* by its 350 μm emission, through blank deep observations of the Boötes field in a program designed to search efficiently for new sources at 350 μm (the SHARC II Unbiased Deep Survey, SUDS; Khan et al., 2005, in preparation). Verification of the detection is confirmed by coincident sources subsequently identified in the *Spitzer* MIPS 24 μm filter, all four *Spitzer* IRAC filters, and J, K_s, I and R band, enabling us to place constraints on the photometric redshift, luminosity and nature of this source. This Letter

¹ Imperial College London, Blackett Laboratory, Prince Consort Road, London SW7 2AZ, UK

² Observational Cosmology Laboratory (Code 665), NASA / Goddard Space Flight Center, Greenbelt, MD 20771

³ SSAI, Lanham, MD 20706

⁴ NRC

⁵ Steward Observatory, University of Arizona, 933 N. Cherry Avenue, Tucson, AZ 85721

⁶ *Spitzer* Science Center, MC 220-6, 1200 East California Boulevard, Pasadena, CA 91125

⁷ Department of Astronomy, Cornell University, 610 Space Sciences Building, Ithaca, NY 14853-6801

⁸ Harvard Smithsonian Center for Astrophysics, 60 Garden Street MS-66, Cambridge, MA 02138

⁹ National Optical Astronomy Observatory, Tucson, AZ 85719-6732

¹⁰ Jet Propulsion Laboratory, California Institute of Technology, MC 169-327, 4800 Oak Grove Drive, Pasadena, CA 91109

¹¹ Department of Astronomy, University of Florida, Gainesville, FL 32611

¹² Deceased

TABLE 1
MULTIWAVELENGTH PHOTOMETRY FOR SSG 1

Observed wavelength	Flux density	Instrument–Survey
X-ray (0.5–7 keV)	$< 4 \times 10^{-15}$ c.g.s	<i>Chandra</i> –XBoötes
4220 Å	$< 0.1 \mu\text{Jy}$	KPNO–NDWFS
6590 Å	$1.0 \pm 0.1 \mu\text{Jy}$	KPNO–NDWFS
8081 Å	$3.1 \pm 0.2 \mu\text{Jy}$	KPNO–NDWFS
1.24 μm	$10.5 \pm 1.1 \mu\text{Jy}$	KPNO–FLAMEX
2.16 μm	$42.0 \pm 1.4 \mu\text{Jy}$	KPNO–FLAMEX
3.6 μm	$80.0 \pm 2.9 \mu\text{Jy}$	<i>Spitzer</i> IRAC–Shallow
4.5 μm	$65.8 \pm 3.6 \mu\text{Jy}$	<i>Spitzer</i> IRAC–Shallow
5.8 μm	$55.3 \pm 17.3 \mu\text{Jy}$	<i>Spitzer</i> IRAC–Shallow
8.0 μm	$81.7 \pm 15.1 \mu\text{Jy}$	<i>Spitzer</i> IRAC–Shallow
24 μm	$0.61 \pm 0.04 \text{ mJy}$	<i>Spitzer</i> MIPS–IRS/MIPS GTO
70 μm	$< 40 \text{ mJy}$	<i>Spitzer</i> MIPS–IRS/MIPS GTO
160 μm	$< 100 \text{ mJy}$	<i>Spitzer</i> MIPS–IRS/MIPS GTO
350 μm	$23.2 \pm 7.9 \text{ mJy}$	SHARC II–SUDS
21 cm	$< 63 \mu\text{Jy}$	Westerbork–Deep 1.4 GHz

presents these fluxes, plus important flux upper limits in other bands, to characterize this source, and with this understanding we consider the implications for other sources that may be discovered at 350 μm .

2. OBSERVATION

Eight hours of data were obtained using the Second Generation Submillimeter High Angular Resolution Camera (SHARC II) at the Caltech Submillimeter Observatory (CSO) on Mauna Kea, Hawai‘i, in January and March 2004. SHARC II is a 350 μm -optimized camera (Dowell et al. 2003) built around a 12×32 element close-packed bolometer array (Moseley et al. 2004). It achieves a point-source sensitivity of $\sim 1 \text{ Jy Hz}^{-1/2}$ in good weather. The 384 pixels of the SHARC II array image a region of around $1.0' \times 2.5'$ on the sky. Its filled absorber array provides instantaneous imaging of the entire field of view, sampled at roughly 2.5 pixels per nominal beam area. The beam profile was measured on known compact sources, and was verified to be within three per cent of the diffraction-limited beamwidth of $8.5''$. All observations were taken using the Dish Surface Optimisation System (Leong et al. 2003), which corrects for the primary mirror deformation as a function of zenith angle, to improve the telescope efficiency and the pointing.

For these data the in-band zenith atmospheric opacity ($\tau_{350 \mu\text{m}}$) ranged from 1.0 to 1.4, corresponding to a zenith transmission of around 30 per cent. Our observations were centred on the Boötes Deep Field (de Vries et al. 2002), at position RA = $14^{\text{h}}32^{\text{m}}5.75^{\text{s}}$, Dec = $34^{\circ}16'47.5''$ (J2000).

The data were reduced using the standard CSO reduction software, CRUSH (Kovács, 2005, in preparation). This software implements a self-consistent least-squares algorithm to solve for the celestial emission, taking into account instrumental and atmospheric contributions to the signal.

The sky map is calibrated with the flux and point spread function based on observations of Callisto taken throughout the observing period at similar elevations.

3. RESULTS

An oversampled χ^2 fit is used to determine the position of the source and the flux per beam. The best-fitting position is at $14:32:06.65 \pm 0.24 +34:16:13.4 \pm 3.4$ (J2000) (quoting 3σ po-

TABLE 2
COINCIDENT DETECTION POSITIONS AND PROBABILITY OF ACCIDENTAL OVERLAP WITHIN THE 99% CONFIDENCE REGION OF SSG 1

Position (J2000) RA	Dec	Band	P(Accidental Overlap)
14:32:06.61	+34:16:12.0	R	9.5%
14:32:06.55	+34:16:11.6	K_s	2.9%
14:32:06.58	+34:16:12.0	3.6 μm	9.4%
14:32:06.60	+34:16:11.5	24 μm	0.2%
14:32:06.65	+34:16:13.4	350 μm	n/a

sition uncertainties), with a flux per beam of $23.2 \pm 7.9 \text{ mJy}$ (the 1σ uncertainty comprises the background noise, primary calibrator and gain calibration errors). The signal-to-noise in the detection is 3.6. The additional photometry for SSG 1 (Table 1) is from the *Chandra* XBoötes survey (Murray et al. 2005), NOAO-NDWFS (Jannuzi & Dey 1999), FLAMEX (Elston et al., 2005, in preparation), *Spitzer*-IRAC Shallow survey (Eisenhardt et al. 2004), *Spitzer*-MIPS (IRS and MIPS GTO teams) and the Westerbork deep 1.4 GHz survey (de Vries et al. 2002). The upper limits are quoted to 3σ . The corresponding multiwavelength positions and probability of coincident detection are given in Table 2.

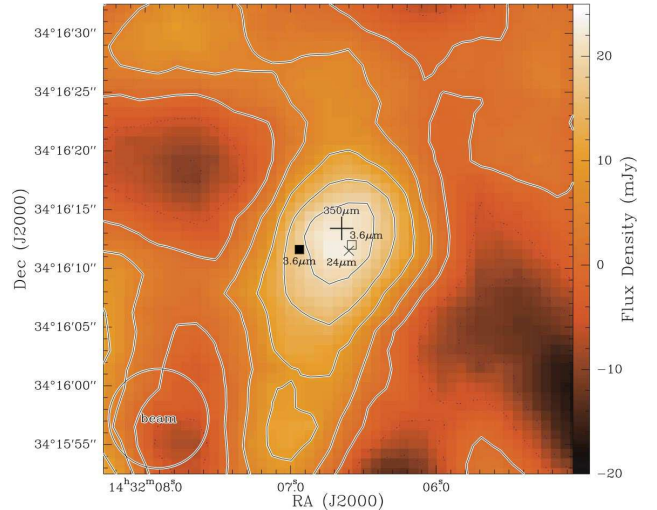


FIG. 1.— 350 μm continuum emission map of SSG 1, as imaged by SHARC II. The SHARC II (plus) and MIPS position (cross) are overplotted, along with the resolved IRAC 3.6 μm positions of SSG 1 (open square) and SSG 1E (filled square). The contours are in levels of 5 mJy/beam.

Within the 99% 350 μm confidence region there are two candidate sources resolved in the optical and NIR bands (Figure 1). We assume that the optical-NIR counterpart of SSG 1 is the source coincident with the MIPS 24 μm detection. The source to the east of this (at IRAC position RA = $14^{\text{h}}32^{\text{m}}6.94^{\text{s}}$, Dec = $+34^{\circ}16'11.6''$ /J2000) is not detected by MIPS, and is designated as SSG 1E for the purposes of this Letter.

4. CONSTRAINING THE NATURE OF SSG 1

Using the fluxes presented in Table 1, we can use several methods to constrain the redshift, reddening, infrared luminosity and dust temperature of SSG 1. It can be seen in Fig-

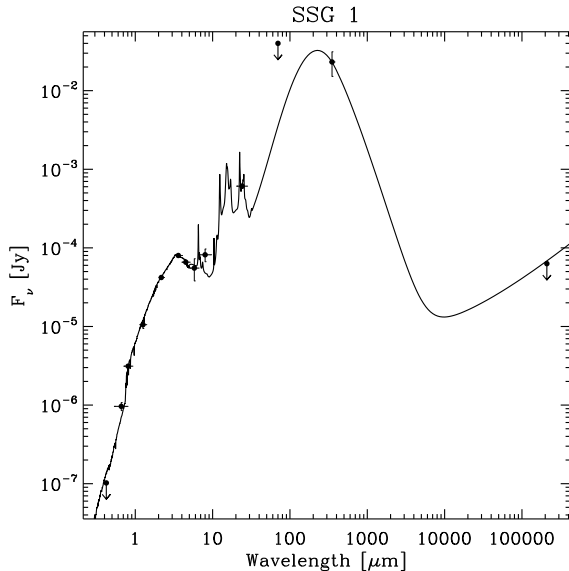


FIG. 2.— Best-fitting observing frame SED to SSG 1 from STARDUST2

TABLE 3
BEST-FITTING PHOTOMETRIC REDSHIFTS AND EXTINCTION FOR
SSG 1 AND SSG 1E WITH IMPZ AND STARDUST2

Source	Photometric Redshift	Model	A_V
SSG 1	$1.0^{+0.10}_{-0.05}$	IMPZ	2.6 ± 0.2
	$0.99^{+0.04}_{-0.03}$	STARDUST2	2.2 ± 0.09
SSG 1E	1.0 ± 0.05	IMPZ	0.5 ± 0.1

ure 2 that the optical-NIR SED of SSG 1 is characterized by a prominent bump associated with the continuum emission of the stellar populations. This bump peaks at $1.6 \mu\text{m}$ in the rest-frame, providing a very good constraint on the redshift, and also indicates SSG 1 is more likely to be starburst rather than AGN-dominated (which are usually associated with a featureless power-law spectrum; see, e.g., Egami et al. 2004).

IMPZ (Babbedge et al. 2004) uses only the optical-NIR photometry when fitting templates with Bayesian statistics. The best-fitting redshifts are $z=1.0^{+0.1}_{-0.05}$ for SSG 1 and $z=1.0 \pm 0.05$ for SSG 1E respectively (1σ), and are listed in Table 3. It is worth noting that if, as IMPZ suggests, both galaxies are at the same distance, and interacting, it would make the SSG pair a widely separated interacting ULIRG system (a local example of which is IRAS 09111–1007; Khan et al. 2005).

STARDUST2 (Chen et al., 2005, in preparation) uses a mid-IR to radio spectral library constrained by the IR-radio correlation and a variety of local, *IRAS*, *ISO* and SCUBA color-color correlations in addition to a stellar synthesis model for the FUV to NIR window (Devriendt et al. 1999). This provides a simultaneous constraint on the thermal dust emission as well as the redshift. The effective dust temperature is found following the methodology given in Chapman et al. (2002; 2005). The model assumes $H_0 = 70 \text{ km s}^{-1} \text{ Mpc}^{-1}$, $\Omega_m = 0.3$, and $\Omega_\Lambda = 0.7$, and that a single component is responsible for both the optical and IR emission. Because of

the degeneracy in fitting T_{dust} and the Total-IR Luminosity, L_{TIR} (8–1100 μm), it is the 350 μm flux in conjunction with the radio upper limit that constrains the infrared luminosity. The radio upper limit (Table 1) is used to find χ^2 as follows:

$$\chi^2 = \sum \chi_i^2 \text{ with the radio } \chi_i^2 \text{ term being}$$

$$\chi_{\text{radio}}^2 = [f_\nu(1.4 \text{ GHz}) - 3\sigma]^2 / \sigma^2, f_\nu(1.4 \text{ GHz}) > 3\sigma \\ = 0, f_\nu(1.4 \text{ GHz}) \leq 3\sigma$$

where f_ν is the modeled spectral energy distribution and 3σ is the radio upper limit listed in Table 1.

The best-fitting model for SSG 1 from STARDUST2 returns a redshift of $0.99^{+0.04}_{-0.03}$ (all errors are quoted to 1σ ; note: STARDUST2 uses the longer wavelengths, in addition to the optical-NIR photometry, to fit the extinction given in Table 3). This model also gives a dust temperature of $30.3 \pm 4.5 \text{ K}$, and a $\log(L_{\text{TIR}})$ of $12.02^{+0.22}_{-0.24} L_\odot$, with 88% of the total bolometric luminosity radiated at wavelengths longward of $5 \mu\text{m}$. The predicted 850 μm flux is $2.7^{+1.7}_{-0.7} \text{ mJy}$.

Other redshift estimates were independently obtained following an approach that mostly relies on the fit of the $1.6 \mu\text{m}$ feature (see, e.g., Le Floc'h et al. 2004). In agreement with the results derived from IMPZ and STARDUST2, these fits of the stellar bump led to a redshift $z \sim 1$ using the photometric Arp220 SED, and $z=1.25 \pm 0.25$ using various templates from the library of Devriendt et al. (1999).

We also use the radio-submillimeter correlation to estimate a minimum redshift for the source, as the radio flux is unlikely to be significantly AGN-enhanced. Formally, these correlations should be used as a statistical redshift indicator, so with that caveat we present the minimum redshift of SSG 1 based on the 1.4 GHz upper limit (Table 1) and an 850 μm flux derived from the best-fitting STARDUST2 SED (Figure 2). Using the relations of Dunne, Clements & Eales (2000) and Carilli & Yun (2000a; 2000b) we get z_{min} of 1.2 and 1.5 respectively.

The photometric redshift is more secure than the radio-submillimeter correlation since the latter is prone to systematics caused by uncertain dust temperatures (see Clements et al. 2004).

5. DISCUSSION

The $(R-K_s)_{\text{Vega}}$ color of 5.7 for SSG 1 classifies it as an Extremely Red Object (ERO), and both IMPZ and STARDUST2 find this object to be highly reddened (Table 3). At least a third of the SMG population can be classified as EROs (Smail et al. 2002; Webb et al. 2004; Frayer et al. 2004), which comprise two classes of galaxies: elliptical and dusty star-forming luminous infrared galaxies (but a significant submillimeter flux is usually indicative of the latter class). EROs are thought to comprise a significant fraction of the cosmic star formation density at redshifts of one and higher (Cimatti et al. 2002), the epoch by which the majority of the universe's star formation has taken place (Dickinson et al. 2003; Rudnick et al. 2003).

Determining the effective dust temperature of the source allows us to estimate the total fraction of the bolometric luminosity that is reprocessed by the dust. Our effective dust temperature from STARDUST2 is $30.3 \pm 4.5 \text{ K}$, which, with our total infrared luminosity of $1.0 \times 10^{12} L_\odot$, allows us to directly compare SSG 1 with *IRAS* and SCUBA-selected ULIRGs in the L vs T diagram of Blain et al. (2004). We find that SSG 1 is warmer than an equivalent luminosity SMG from the Chapman et al. (2003; 2005) high redshift sample, and cooler

than the *IRAS* moderate redshift counterparts of Stanford et al. (2000). Instead, it is similar to the intermediate redshift *ISO* sample of Garrett (2002).

The notion of SSG 1 being an *ISO* ULIRG analog is further reinforced by the best-fitting 60-100 μm colors from STAR-DUST2, of which the closest template is FN1-40, an *ISO* cold ($T_{\text{dust}}=25.7\text{ K}$) ULIRG at $z=0.45$ (Chapman et al. 2002). The 850 μm flux ($\sim 3\text{ mJy}$) predicts SSG 1 to be fainter than the majority of SCUBA-selected SMGs ($S_{850} \geq 5\text{ mJy}$, due to survey and instrument limitations). We conclude that SSG 1 is more like *ISO*-selected ULIRGs rather than the SCUBA-selected SMGs.

6. CONCLUSION

We report the detection of the first short-wavelength submillimeter-selected galaxy (SSG 1) and present optical, NIR and IR photometry which we use to constrain the redshift, luminosity and dust temperature of this source. The photometric redshift estimators are all in agreement, producing a best-fitting redshift of ~ 1 . The dust temperature of $30.3 \pm 4.5\text{ K}$ and luminosity of $1.0 \times 10^{12} L_{\odot}$ make SSG 1 an analog of intermediate redshift *ISO*-selected ULIRGs rather than high redshift SCUBA-selected SMGs.

If there exists a population of galaxies with properties similar to SSG 1, in a redshift space between *ISO* and SCUBA, it may be argued that observations at 350 μm , in conjunction with the current *ISO*, *Spitzer* and SCUBA samples, could describe the IR-luminous population from $0.3 < z < 4.0$ (although the SCUBA-selected galaxies will be more luminous). Not only would this population bridge the gap in redshift space, but also the gap in “dust temperature space” (and consequently “dust mass space”). SHARC II thus complements SCUBA in revealing warmer SMGs that might be missed oth-

erwise. Furthermore, finding the lower luminosity SMGs is necessary for an accurate understanding of the submillimeter luminosity function.

From our understanding of the first 350 μm -selected object, SSG 1, we infer that observations at 350 μm , far from being superfluous to SCUBA, will be of great use in determining the nature and evolution of the luminous infrared galaxy population.

7. ACKNOWLEDGEMENTS

The Caltech Submillimeter Observatory is supported by NSF contract AST-0229008. This work is based in part on observations made with the *Spitzer* Space Telescope, which is operated by the Jet Propulsion Laboratory, California Institute of Technology under NASA contract 1407. This work made use of images and data products provided by the NOAO Deep Wide-Field Survey (Jannuzi & Dey 1999), which is supported by the National Optical Astronomy Observatory (NOAO). NOAO is operated by AURA, Inc., under a cooperative agreement with the National Science Foundation. The FLAMEX Survey acknowledges support from NOAO and NSF (AST-9875448, AST-0407085, AST-0436681), and technical assistance from S.N. Raines.

We would like to thank the anonymous referee for their insightful comments which have significantly improved this Letter. We also thank Tom Phillips and the CSO for observing time and assistance during our runs, and Darren Dowell, Colin Borys and Attila Kovács for instrument and data reduction support. We express our gratitude to our fellow GSFC co-Is on SUDS: Bob Silverberg and Dave Chuss. We also thank SUDS co-I Rick Arendt for continual support on the data analysis. S.A.K. thanks Jon Gardner, Rob Ivison and Steve Eales for very helpful discussions.

REFERENCES

- Aussel, H., Cesarsky, C. J., Elbaz, D., Starck, J. L., 1999, *A&A*, 342, 313
 Babbedge, T. S. R., et al., 2004, *MNRAS*, 353, 654
 Barger, A. J., Cowie, L. L., Sanders, D. B., Fulton, E., Taniguchi, Y., Sato, Y., Kawara, K., Okuda, H., 1998, *Nature*, 394, 248
 Blain, A. W., Chapman, S. C., Smail, I., Ivison, R., 2004, *ApJ*, 611, 52
 Carilli, C. L., Yun, Min S., 2000, *ApJ*, 530, 618
 Carilli, C. L., Yun, Min S., 2000, *ApJ*, 539, 1024
 Chapman, S. C., Blain, A. W., Smail, I., Ivison, R. J., 2005, *ApJ*, 622, 772
 Chapman, S. C., Blain, A. W., Ivison, R. J., Smail, I. R., 2003, *Nature*, 422, 695
 Chapman, S. C., Smail, I., Ivison, R. J., Helou, G., Dale, D. A., Lagache, G., 2002, *ApJ*, 573, 66
 Cimatti, A., et al., 2002, *A&A*, 381L, 68
 Clements, D., et al., 2004, *MNRAS*, 351, 447
 Connolly, A. J., Szalay, A. S., Dickinson, M., Subbarao, M. U., Brunner, R. J., 1997, *ApJ*, 486, 11
 de Vries, W. H., Morganti, R., Röttgering, H. J. A., Vermeulen, R., van Breugel, W., Rengelink, R., Jarvis, M. J., 2002, *AJ*, 123, 1784
 Devriendt, J. E. G., Guiderdoni, B., Sadat, R., 1999, *A&A*, 350, 381
 Dickinson, M., Papovich, C., Ferguson, H. C., Budavári, T., 2003, *ApJ*, 587, 25
 Dowell C.D., et al., 2003, *SPIE*, 4855, 73
 Dunne, L., Clements, D. L., Eales, S. A., 2000, *MNRAS*, 319, 813
 Eales, S., et al., 1999, *ApJ*, 515, 518
 Egami, E., et al., 2004, *ApJS*, 154, 130
 Eisenhardt, P. R., et al., 2004, *ApJS*, 154, 48
 Elbaz, D., Flores, H., Chaniai, P., Mirabel, I. F., Sanders, D., Duc, P.-A., Cesarsky, C. J., Aussel, H., 2002a, *A&A*, 381, 1
 Elbaz, D., Cesarsky, C. J., Chaniai, P., Aussel, H., Franceschini, A., Fadda, D., Chary, R. R., 2002b, *A&A*, 384, 848
 Fixsen, D. J., et al., 1998, *ApJ*, 508, 123
 Frayer, D. T., et al., 2004, *ApJS*, 154, 137
 Gabasch, A., et al., 2004, *ApJ*, 616, L83
 Garrett, M. A., 2002, *A&A*, 384, L19
 Guiderdoni, B., Hivon, E., Bouchet, F. R., Maffei, B., 1998, *MNRAS*, 295, 877
 Holland, W. S., et al., 1999, *MNRAS*, 303, 659
 Hughes, D. H., et al., 1998, *Nature*, 394, 241
 Jannuzi, B. T., Dey, A., 1999, in "Photometric Redshifts and the Detection of High Redshift Galaxies", ASP Conference Series, Vol. 191, Edited by R. Weymann, L. Storrie-Lombardi, M. Sawicki, and R. Brunner. ISBN: 158381-017-X, p. 111
 Joseph R.D., Wright G.S., 1985, *MNRAS*, 214, 87
 Khan, S.A., Benford, D.J., Clements, D.L., Moseley, S.H., Shafer, R.A., Sumner, T.J., 2005, *MNRAS*, 359L, 10
 Le Floc'h, E., et al., 2004, *ApJS*, 154, 170
 Leong, M., et al., 2003, <http://puuoo.caltech.edu/dsos/DSOSAMOSpaper.pdf>
 Lilly, S.J., Le Fèvre, O., Hammer, F., Crampton, D., 1996, *ApJ*, 460, 1
 Madau, P., Ferguson, H. C., Dickinson, M. E., Giavalisco, M., Steidel, C. C., Fruchter, A., 1996, *MNRAS*, 283, 1388
 Moseley S.H., Allen C.A., Benford D., Dowell C.D., Harper D.A., Phillips T.G., Silverberg R.F., Staguhn J., 2004, *NIMPA*, 520, 417
 Murray, S.S., et al., 2005, *astro-ph/0504084*
 Puget, J.-L., Abergel, A., Bernard, J.-P., Boulanger, F., Burton, W. B., Desert, F.-X., Hartmann, D., 1996, *A&A*, 308, L5
 Rowan-Robinson, M., et al., 1999, *The Universe as Seen by ISO*. Eds. P. Cox & M. F. Kessler. ESA-SP 427., p. 1011
 Rudnick, G., et al., 2003, *ApJ*, 599, 847
 Simpson, C., Dunlop, J. S., Eales, S. A., Ivison, R. J., Scott, S. E., Lilly, S. J., Webb, T. M. A., 2004, *MNRAS*, 353, 179
 Smail, I., Owen, F. N., Morrison, G. E., Keel, W. C., Ivison, R. J., Ledlow, M. J., 2002, *ApJ*, 581, 844
 Smail, I., Ivison, R. J., Blain, A. W., 1997, *ApJ*, 490L, 5
 Soifer B.T., Neugebauer G., Houck J.R., 1987, *ARA&A*, 25, 187
 Soifer B.T., et al., 1984, *ApJ*, 278L, 71
 Stanford, S. A., Stern, D., van Breugel, W., De Breuck, C., 2000, *ApJS*, 131, 185
 Steidel, C. C., Adelberger, K. L., Giavalisco, M., Dickinson, M., Pettini, M., 1999, *ApJ*, 519, 1
 Webb, T. M. A., Brodwin, M., Eales, S., Lilly, S. J., 2004, *ApJ*, 605, 645
 Yan, L., et al., 2004, *ApJS*, 154, 75